Shuwen Zhou
Qingyun Wang ✉
Jinshuang Liu

https://doi.org/10.21278/TOF.461019420
ISSN 1333-1124
eISSN 1849-1391

CONTROL STRATEGY AND SIMULATION OF THE REGENERATIVE BRAKING OF AN ELECTRIC VEHICLE BASED ON AN ELECTROMECHANICAL BRAKE

Summary

The electromechanical brake (EMB) has very broad prospects for application in the automotive industry, especially in small- and medium-sized vehicles. To extend the endurance range of pure electric vehicles, a regenerative braking control strategy combined with an electromechanical brake model is designed that divides the braking modes according to the braking intensity and controls the regenerative braking force based on fuzzy theory. Considering a front-wheel-drive pure electric vehicle equipped with a floating clamp disc electromechanical brake as the research object, a structural form of electromechanical brake is proposed and a mathematical model of the electromechanical brake is built. Combined with the relevant influencing factors, the regenerative braking force is limited to a certain extent, and the simulation models of the electromechanical brake and the regenerative braking force distribution control strategy are built in MATLAB/Simulink. Co-simulation in MATLAB and AVL CRUISE software is conducted. The simulation results demonstrate that the braking energy recovery rate of the whole vehicle with the fuzzy control strategy put forward in this paper is 28.9% under mild braking and 34.11% under moderate braking. The control method substantially increases the energy utilization rate.

Key words: *Regenerative braking; Electromechanical brake device; Co-simulation; Pure electric vehicle*

1. Introduction

Brake energy recovery is of substantial importance in electric vehicles, not only for recovering kinetic energy to improve the cruising range but also for reducing the brake system burden to improve vehicle safety and to extend the life of the brake system [1]. Since braking energy recovery and mechanical braking force are closely related, the control strategy of electric braking needs to be based on the control of the mechanical braking torque to achieve the regenerative braking effect of the vehicle braking system [2].

In a regenerative braking system, it is typically necessary to let the motor become an electric generator by using the vehicle's momentum as the mechanical energy for putting the motor into reverse. Once the motor is operating in reverse, the generated electricity will feed the battery or capacitor and can be used to drive the vehicle again. Regardless of the vehicle

design, the motor/generator (M/G) must have a mechanical connection to the drivetrain. In electric vehicles, each wheel may have a separate M/G or a central M/G that is connected to the drivetrain. In a hybrid vehicle, the M/G can be a separate component [3].

In the control of the vehicle brake operation, rational distribution between the mechanical and regenerative braking forces is necessary. As a result, various control strategies and control algorithms have been designed. Ferreira et al. put forward an energy system control strategy on the basis of fuzzy logic monitoring [4]. Through specific simulation and experimental research, the results make it clear that fuzzy control is an appropriate energy system management and control strategy. Bai et al. established the state space model of regenerative braking of a pure electric vehicle equipped with a permanent magnet synchronous motor and designed H_ robust controller [5]. The results show that the controller can effectively combine motor braking with mechanical braking, reducing the influence of initial speed and driving mode changes. Compared with some traditional controllers, this one has a faster response speed and smaller tracking error. Fazeli et al. studied the control characteristics of an improved adaptive sliding mode controller for regenerative braking torque which is produced by a new type of cam-air hybrid engine [6]. The basic subassembly of the new synovial controller model is obtained from the estimated inverse dynamic model which is directly generated by the hybrid engine. The controller is also used to estimate the variation characteristics of each parameter and to compensate system interference in the dynamic system. Saeks et al. designed a system consisting of four independent adaptive controllers, which are respectively used to control driving direction, vehicle speed, sideslip, and the energy system [7]. The results show that the power variation of this controller is in the specific estimation range, and the same controller can be used under different road conditions and loads, using the same parameters. The instantaneous optimization strategy adopted by Sciarretta et al. can effectively design the real-time power distribution control of hybrid electric vehicles [8]. There is no need to predict the future, and only a small number of control parameters are needed, which change with the driving conditions. The instantaneous cost function can be minimized and evaluated by choosing appropriate torque distribution control variables.

Laldin of Purdue University and others proposed a control algorithm for a hybrid energy system of a pure electric vehicle [9]. The control algorithm performs predictive control based on the state of the energy storage system. The system combines the advantages of the super capacitor and battery. The experimental results indicate that compared with the traditional energy storage system, the energy storage system using the optimal control algorithm can recover more regenerative braking energy. Indian scholar Khastgir proposed a regenerative braking control strategy according to a new assembly configuration [10]. The pure electric vehicle used as the research object works on rear-wheel drive, and the regenerative braking force is used for the front wheels. This control strategy does not need to change the traditional braking system. The simulation results indicate that the regenerative braking control strategy can recover about 30% of total braking energy. Li et al. put forward a braking control strategy for pure electric vehicles on the basis of ECE regulations and the I curve. Simulink and ADVISOR software are used to establish a simulation model for the joint control strategy of the automobile and energy recovery. The research is aimed at the traditional hydraulic brake system. The ECE and f-line are directly selected in the process of braking force distribution, so that the braking energy recovery effect is not very satisfactory [11]. Shi et al. studied the distribution method of regenerative braking force and mechanical friction braking force on the front and rear wheels which can recover more energy but did not fully consider the restrictions of various factors affecting energy recovery [12]. Liu et al. comprehensively considered the limitation of electric power and other influencing factors, combined with the safe braking range to distribute the braking force [13]. However, this kind of method adopts the safe braking range under ideal conditions, which has great theoretical value but needs to be improved in practical application.

Compared to the traditional braking system, the electromechanical brake is more advantageous in terms of the braking force response time [14]. A braking mode based on the braking intensity and a braking control strategy on the basis of fuzzy theory are proposed. Considering an electric vehicle equipped with an electromechanical brake (EMB) as the research object, the mathematical model of EMB and the corresponding simulation model of the braking control strategy are established. The proposed control strategy is evaluated via co-simulation using MATLAB and AVL CRUISE.

2. Regenerative Braking System based on EMB

The structure of the regenerative braking system of an electric vehicle is illustrated in Fig. 1. This car is an EMB-equipped front-axle-drive electric car. Braking torque from the motor and the transmission structure can be applied to the front axle, while the braking force of the rear axle can only be provided by friction torque of the EMB actuator. When the pure electric vehicle brakes, the vehicle brake control unit (BCU) receives road condition signals from sensors, calculates the optimal regenerative braking force generated by the motor and the optimal EMB friction braking force in real time according to the states of the battery and the motor, and transmits the signals to the motor and the EMB actuators to adjust the regenerative braking force provided by the motor and the caliper clamping force of the front and rear axle EMB in real time. When the pure electric vehicle brakes, the electrical energy generated by the generator can be directly supplied to the EMB actuator and the electrical energy of the storage battery is used as a supplement. If the generator generates more electricity than the EMB system requires, the excess electricity can be stored in the battery. A flow diagram of the regenerative braking system based on EMB is illustrated in Fig. 2.

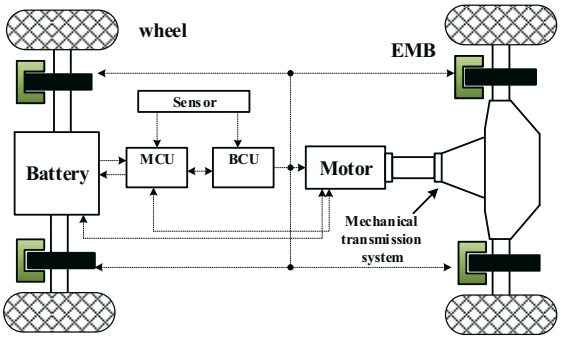

Fig. 1 Structure of the regenerative braking

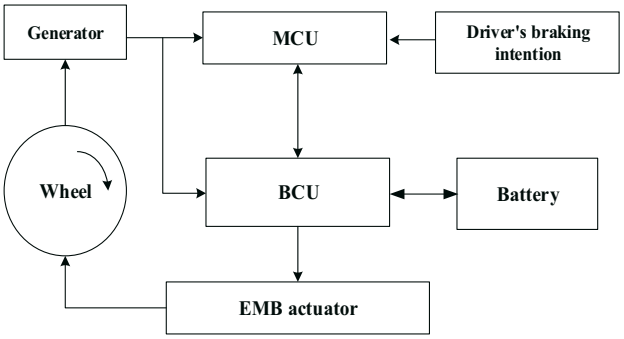

Fig. 2 Flow diagram of the regenerative braking

2.1 Electromechanical Brake

As illustrated in Fig. 3(a), the electromechanical brake is composed of a DC servo motor, a gearbox, a ball screw, a brake disc, a gap adjusting shim, and a return spring, among other components. The DC servo motor provides power. Composed of two-stage straight cylindrical gears, the gearbox is used to reduce the speed and increase the torque [15]. The ball screw is used to convert the rotary motion of the motor into the linear motion of the brake piston. The adjusting shim and return spring are used to achieve brake release. The torque generated by the servo motor is converted into force for pushing the brake piston to move linearly through the gearbox and the ball screw. By comparison with the traditional hydraulic brake system, the electromechanical brake is more compact due to the absence of a huge vacuum booster mechanism. In addition, the power of EMB comes from the servo motor; hence, EMB is safe, reliable and flexible [16]. More importantly, the electrical energy that is generated by the generator in the braking process can be directly supplied to the EMB actuator, which not only reduces the energy loss in the charging and discharging process [17] but also reduces the number of charges and discharges of the storage battery to extend the service life of the storage battery [18].

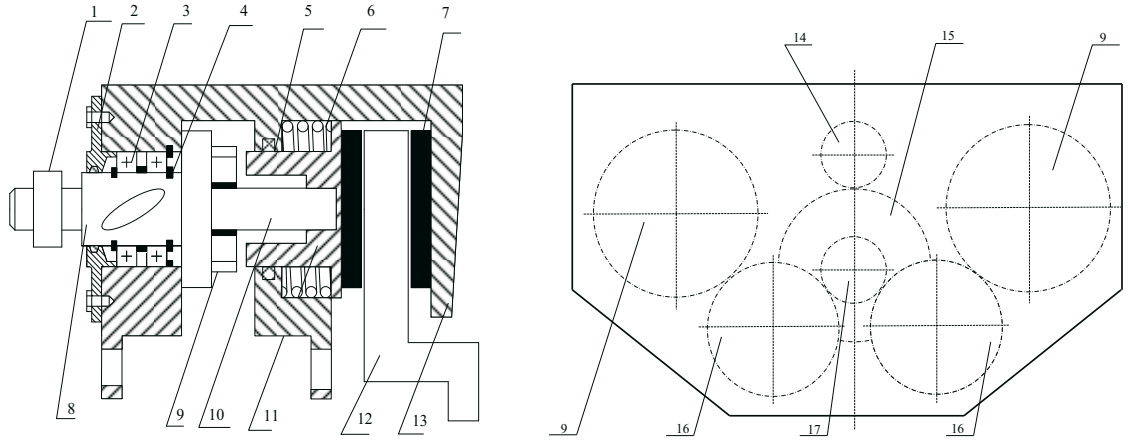

(a) Structure of EMB (b) Structure of the Gear Box

(1. Limit block, 2. Bearing end cover, 3. Bearing, 4. Retaining ring, 5. Piston seal ring, 6. Return spring, 7. Friction plate, 8. Ball screw nut, 9. Power output large gear, 10. Ball screw, 11. Brake piston, 12. Brake disc, 13. Brake caliper body, 14. Power input pinion, 15. Intermediate shaft gear, 16. Transition idler, and 17. Intermediate shaft pinion)

Fig. 3 Electromechanical brake

2.2 Mathematical Modelling of the EMB Actuator

To study the regenerative braking system based on EMB, it is necessary to obtain a mathematical model of EMB. Considering the floating caliper disc EMB brake as an example, its motor, deceleration and torque increasing mechanism, motion conversion mechanism and brake disc are modelled.

2.2.1 Modelling of the Drive Motor

In this paper, a brushless DC torque motor is selected and its output torque is converted into pressure that moves the brake clamping pad close to the brake disc. In the process of braking, the motor is in a state of continuous locked rotation. A modified formula for calculating the output torque of the motor in a state of continuous locked rotation is as follows [19]:

$$T_d = 4.89 k_e I_a , \tag{1}$$

where I_a is the locked-rotor current of the motor, which is expressed in A, and k_e is the back electromotive force coefficient, which is defined as the electromotive force at unit rotation speed and can be calculated from the motor's parameters by the following:

$$k_e = (U_0 - I_0 R_a) / n_0 , \tag{2}$$

where U_0 is the no-load voltage of the motor that is implemented for EMB, which is expressed in V; I_0 is the no-load current of the motor; n_0 is the motor no-load speed, which is expressed in rpm; and R_a is the armature resistance, which is expressed in **Ω**.

2.2.2 Modelling of the Gear Mechanism

As illustrated in Fig. 3(b), the gearbox consists of a two-stage spur gear mechanism for two-stage reduction and torque increase. The torque that is exerted by the deceleration torque increasing mechanism can be expressed as follows:

$$T_g = T_d i_g \eta_g , \tag{3}$$

where T_g is the torque that is generated by the gearbox mechanism, which is expressed in N·m, and i_g and η_g are the total transmission ratio and the transmission efficiency, respectively, of the reduction and torsion increasing mechanism.

2.2.3 Modelling of the Motion Conversion Mechanism

The ball screw converts the rotary motion of the motor and the gearbox into a linear motion. The output of the brake piston that presses the brake disc can be expressed as follows:

$$F_p = \frac{2\pi T_g \eta_s}{P_h}, \tag{4}$$

where η_s is the efficiency of the ball screw drive pair and P_h is the lead of the ball screw, which is expressed in m.

2.2.4 Modelling of the Brake Discs

When the vehicle is braking, the force from the DC servo motor is converted into the pressing force of the brake piston to press the brake disc through the gearbox and the ball screw and the pressing force act on the brake disc to generate the braking torque, which can be expressed as follows:

$$T_b = 2F_p \eta_b R_b \mu_b c_b, \tag{5}$$

where R_b is the effective contact radius of the brake disc and the caliper body, which is expressed in m; μ_b is the friction coefficient of the brake; η_b is the braking efficiency of the brake; and c_b is the specific braking factor.

Combined with the above equation, the braking torque can be expressed as follows:

$$T_b = \frac{4\pi \eta_s \eta_b \eta_g R_b \mu_b c_b i_g (4.89 k_e I_a)}{P_h}. \tag{6}$$

3. Permitted Area for Braking Force Distribution Between Axles

3.1 Distribution of the Braking Force between the Front and Rear Axles

The handling stability of the vehicle and the utilization degree of attachment conditions play a vital role in the distribution of braking force between the front and rear axles of the vehicle in the whole vehicle braking process [20]. As a pure electric vehicle, the working performance of the braking system is affected by many factors, mainly involving the distribution of braking force between axles and whether or not the front and rear wheels are locked. The stable braking and regenerative energy recovery of pure electric vehicles are often contradictory; hence, a regenerative braking control strategy that considers both energy recovery and stable braking is of great significance [21].

To further study the braking force distribution of the car, the force of the car during braking is analysed. To simplify the calculation, the side rolling and sliding of a pure electric vehicle and the rolling moment and inertial moment of the vehicle are ignored, as illustrated in Fig. 4. The moment is calculated at the grounding points of the front and rear wheels respectively to obtain the sum of the supporting forces that are received by the front shafts F_{z1} and the rear shafts F_{z2} from the ground and can be expressed as follows:

$$\begin{cases} F_{z1} = \dfrac{G}{L}(L_b + zh_g) \\ F_{z2} = \dfrac{G}{L}(L_a - zh_g) \end{cases}, \tag{7}$$

where G is the gravity of a pure electric vehicle; F_{z1} and F_{z2} are the supporting reaction forces from the ground on the front axle and the rear axle, respectively; L is the wheelbase of the vehicle, which is expressed in m; and L_a and L_b are respectively the distances from the front and rear axles to the centroid of the pure electric vehicle, in m.

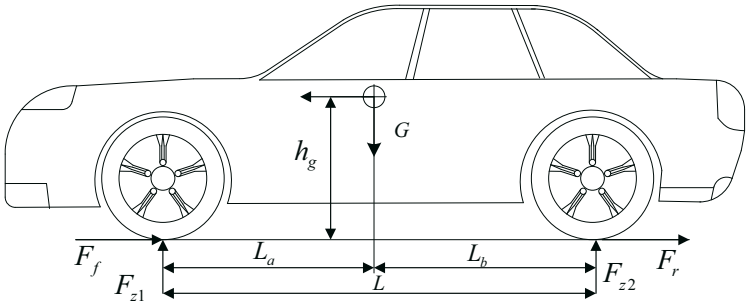

Fig. 4 Kinetic analysis of the vehicle in the braking process

3.2 Permitted Area for the Braking Force Distribution

No matter what the road adhesion coefficient is, the simultaneous locking of the front and rear wheels of the automobile can fully utilize the adhesion conditions and improve braking stability. To lock all wheels of the automobile concurrently, the following conditions must be satisfied:

$$\begin{cases} F_f + F_r = \varphi G \\ \dfrac{F_f}{F_r} = \dfrac{F_{z1}}{F_{z2}} \end{cases}, \tag{8}$$

where φ is the road adhesion coefficient and F_f and F_r are respectively the braking forces acting on the drive shaft and the driven shaft, which are expressed in N.

The ideal curve describes a scenario in which the car makes the most of the adhesion conditions of the ground during braking. This braking force distribution mode corresponds to the scenario in which the front and rear wheels are locked simultaneously. The relationship between the braking forces of the front and rear axles can be obtained by eliminating φ from equations (7) and (8) and can be expressed as follows:

$$F_r = \frac{1}{2}\left[\frac{G}{h_g}\sqrt{L_b^{\,2} + \frac{4h_g L}{G}F_f} - \left(\frac{GL_b}{h_g} + 2F_f\right)\right]. \tag{9}$$

Under the condition that the front wheels are locked and the rear wheels are not locked, the braking force distribution curve of the automobile front and rear axles is defined as the f curve [22].

$$\begin{cases} F_f = \varphi(L_b + zh_g)\dfrac{G}{L} \\ F_r = Gz - F_f \end{cases}. \tag{10}$$

The ECE *R*13 regulation clearly provides the low limit of braking force for the rear axle to participate in vehicle braking from the perspective of satisfying the braking efficiency. Braking regulations stipulate that if a vehicle brakes on a road surface with an adhesion coefficient φ of 0.2 ~ 0.8, the braking strength z must satisfy $z \geq 0.1+0.85(\varphi-0.2)$. Furthermore, the front-axle utilization adhesion coefficient curve should be above that of the rear axle [23]

$$\begin{cases} F_f = \dfrac{z+0.07}{0.85}\dfrac{G}{L}(L_b + zh_g) \\ F_r = Gz - F_f \end{cases}. \tag{11}$$

In summary, the area that is bounded by the ideal curve (*I* curve), the ECE regulation line, the X-axis, and the *f* curve is called the permitted area of the braking force distribution, which is illustrated in Fig. 5. In the working process of the brake assembly of a pure electric vehicle, the braking distribution between the axles must be in this area to ensure braking safety.

4. Braking Force Distribution Control Strategy

4.1 Distribution of the Braking Force between the Front and Rear Axles

Since the front wheels are the driving wheels, the larger the amount of braking force allocated to the front axle during the braking period of a pure electric vehicle, the more braking energy can be reclaimed by the regenerative braking system. However, with the increase of the braking strength, the requirements of ECE R13 braking regulations and braking stabilization must be satisfied [24]. In view of the above problems, the specific distribution mode of the front and rear axle braking force is divided into the situations given below.

If the braking strength z is less than z_A, it is stipulated that the braking force at this time is entirely provided by the front axle. If $z_A \leq z < z_{B1}$, the distribution curve of the braking force between the axles is on the basis of section AB_1 of the ECE regulation curve. If $z_{B1} \leq z < z_C$, the front-axle and rear-axle braking force is allocated in accordance with B_1C, where B_1C_1 is parallel to the f curve and, compared with the f curve in the permitted area mentioned above, the front-axle braking force in B_1C_1 is 95% of that. If the braking intensity z exceeds z_C, the braking force allocation curve of the front and rear axles is on the basis of the I curve, where z_A, z_{B1}, and z_C correspond to the braking strengths at points A, B_1 and C, respectively [25], in Fig. 5.

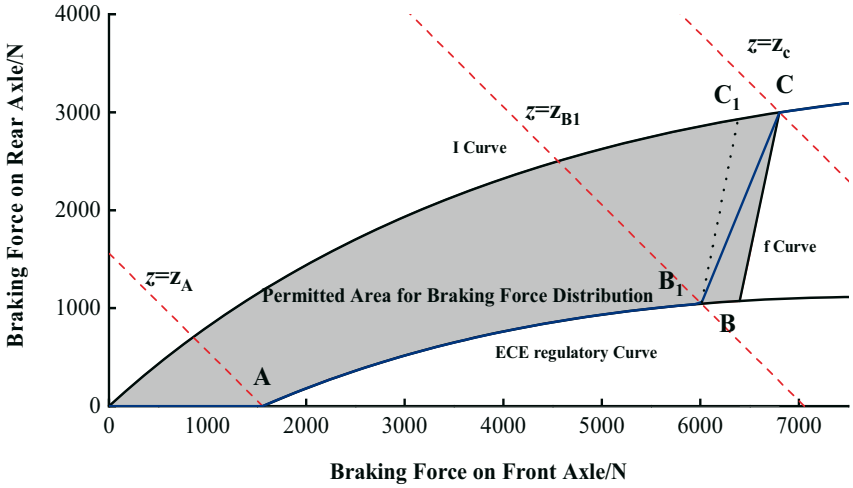

Fig. 5 Braking force distribution

In summary, it is concluded that the distribution relation of the braking force of the front and rear axles can be expressed as follows:

$$F_f = \begin{cases} Gz & , z < z_A \\ \dfrac{z+0.07}{0.85} \cdot \dfrac{G}{L} \cdot \left(L_b + zh_g\right) & , z_A \le z < z_{B_1} \\ 0.228Gz + 3981 & , z_{B_1} \le z < z_C \\ z \cdot \dfrac{G}{L} \cdot \left(L_b + zh_g\right) & , z \ge z_C \end{cases} \tag{12}$$

$$F_r = Gz - F_f \,. \tag{13}$$

4.2 Distribution of the Regenerative Braking Force

After determining the total braking force demand under certain braking conditions and the distribution relationship of the braking force between the axles, it is necessary to determine the share of the regenerative braking force in the braking force of the driving axle. The distribution of the motor braking force in the braking process is nonlinear, complex, and random, and is difficult to control through a mathematical model from the perspective of classical control theory [26]. Control theory based on fuzzy mathematics is highly suitable for the regenerative braking torque distribution process in the braking process and a new method is proposed which accepts the battery *SOC*, real-time braking strength *z*, and vehicle speed *v* as inputs. The three input parameters are the critical factors which affect braking safety and the energy recovery rate. The number of universe, function type, variable range and design of fuzzy rules have a direct impact on the advantages and disadvantages of the control strategy that is put forward in this study. The membership functions are divided into three fuzzy subsets, and trapezoidal functions are selected. The fuzzy controller provides the ratio of the regenerative braking force, which is denoted as k_{reg}. First, in accordance with the characteristics of the input and output variables of the controller, membership functions, which are represented in Fig. 6, are formulated for them. Second, through a large number of test and simulation data, further combined with expert experience, fuzzy rules are designed for the fuzzy controller [27]. In the light of the reasoning rules, the surface rendering of the input-output relationship of the fuzzy controller can be obtained, which is shown Fig. 7.

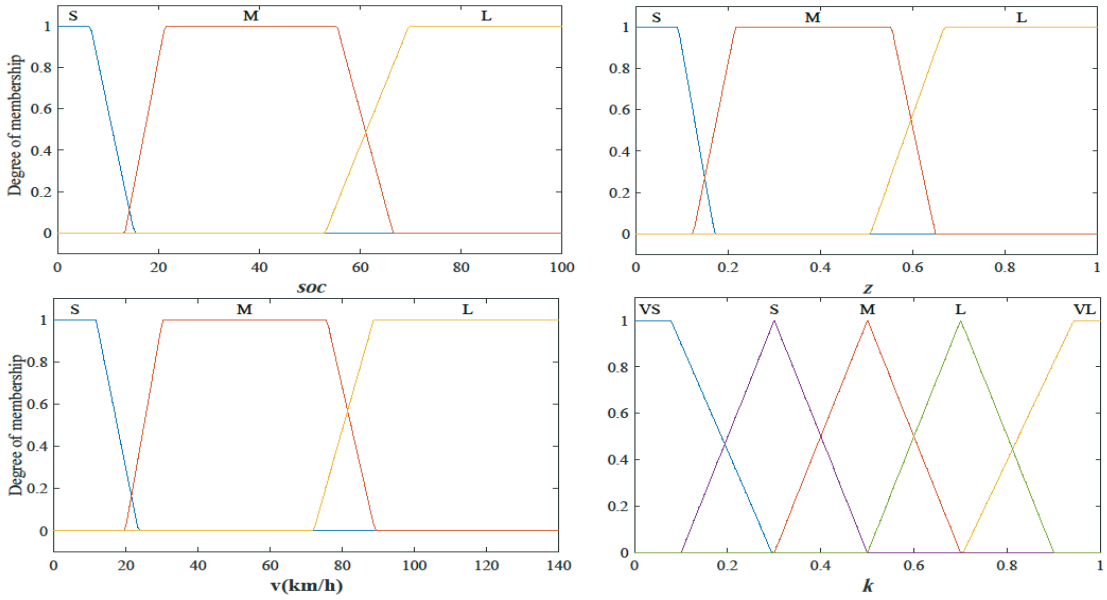

Fig. 6 Membership function

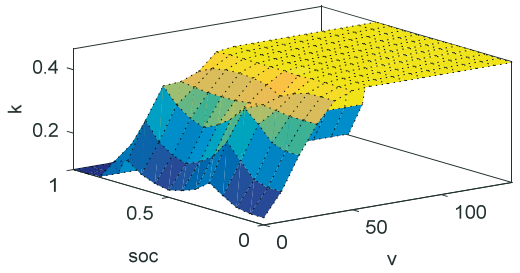

(a) Surface diagram of k changing with SOC and v

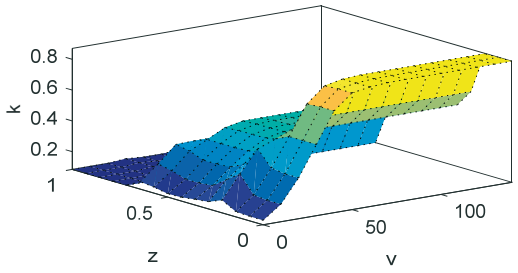

(b) Surface diagram of k changing with z and v

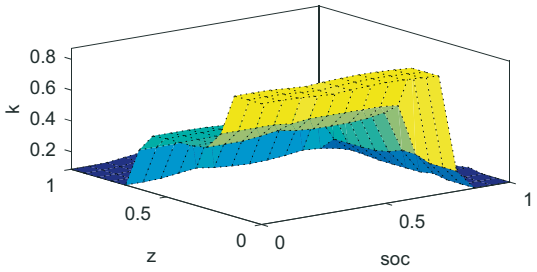

(c) Surface diagram of k changing with z and SOC

Fig. 7 Surface rendering of the input-output relationship

The electric energy generated by regenerative braking is stored in the vehicle-mounted battery pack, and there is an upper limit on the maximum charging current that the battery pack can accept [28]. The charging power of the battery has a vital impact on the safety of the battery. Excessive charging power will directly damage the battery. Generally, the maximum regenerative torque limited by the battery can be described as:

$$T_{reg} \le \frac{9.55\delta P_{bat\_\max}(soc)}{Kn} = \frac{9.55\delta I_{bat\_\max}(U(\text{soc})\text{-}I_{bat\_\max}R_0)\eta_T i_m}{\eta_t \eta_m n} \tag{14}$$

$$\delta = \begin{cases} 1 & , soc < 0.90 \\ 0 & , soc \ge 0.90 \end{cases}, \tag{15}$$

where δ is the limiting factor to prevent the overcharging of the battery pack; R_0 is the total resistance of the battery pack, in Ω; $U(soc)$ is the open circuit voltage of the battery pack, in V; $P_{bat\_\max}(soc)$ is the maximum charging power, in kW; $I_{bat\_\max}$ is the maximum charging current of the battery pack, in A; n is the motor speed, in r/min; η_T is the vehicle transmission efficiency; i_m is the transmission ratio; η_m and η_t respectively represent the generating and the charging efficiency.

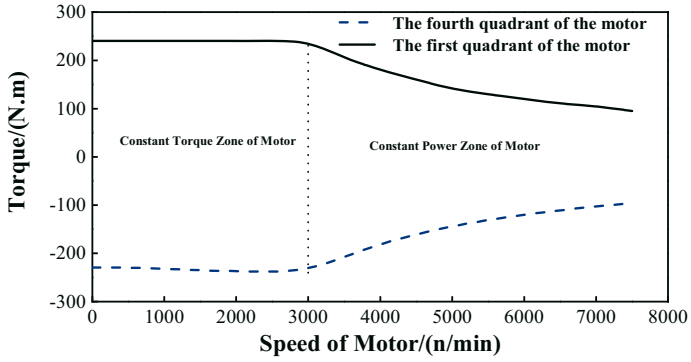

Fig. 8 Motor speed-torque characteristic curve

The working characteristic curve of the motor is shown in Fig. 8. According to the speed-torque characteristic curve, the maximum regenerative braking force that the motor can provide can be obtained, as expressed in equation (16):

$$F_{avaliable}=\begin{cases}0 & ,\ 0\le n<n_{\min}\\ T_{\max}i_m\eta_T/r & ,\ n_{\min}\le n<n_0\\ 9550P_{\max}i_m\eta_T/nr & ,\ n\ge n_0\end{cases}. \tag{16}$$

Finally, in consideration of the impact of the battery *SOC*, the braking strength *z* and the vehicle speed *v*, correction coefficients $\boldsymbol{k_{SOC}}$, $\boldsymbol{k_v}$ and $\boldsymbol{k_z}$ are introduced and are shown in Fig. 9.

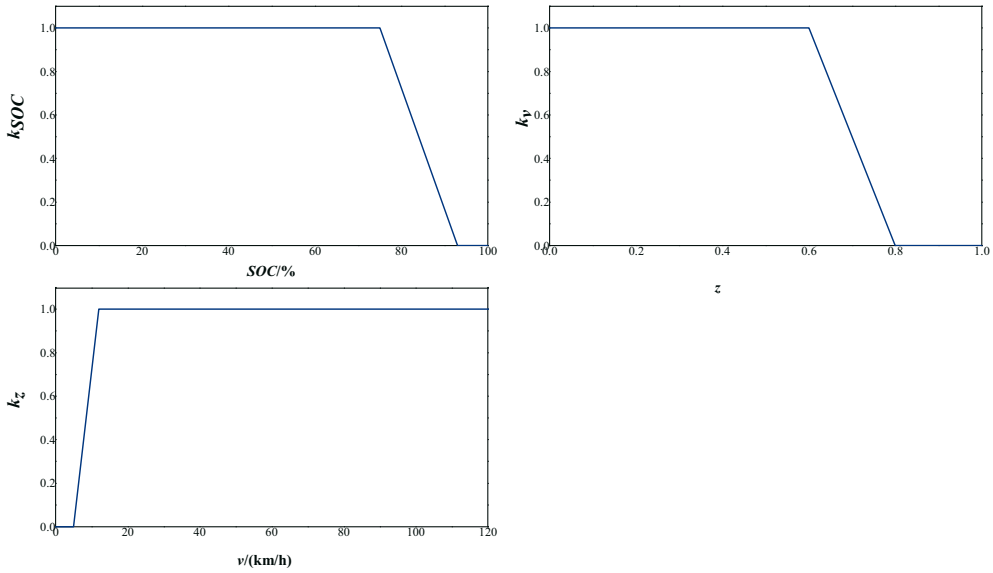

Fig. 9 Correction coefficient

(1) If the battery's electric quantity is too high, the motor does not provide braking torque because bubbles will precipitate if the battery's SOC is too high for charging. To protect the battery, a correction coefficient $\boldsymbol{k_{SOC}}$ is introduced. If the SOC is less than 75%, $\boldsymbol{k_{SOC}}$ is 1; if the SOC is greater than 93%, $\boldsymbol{k_{SOC}}$ is 0; and if the SOC is between 75% and 93%, $\boldsymbol{k_{SOC}}$ decreases linearly from 1 to 0.

(2) If the vehicle speed *v* is too low, the motor speed is low; thus, the back electromotive force of the motor is also low, which will result in limited power generation. If v is less than 5 km/h, $\boldsymbol{k_v}$ is 0; if the vehicle speed is greater than 12, $\boldsymbol{k_v}$ is 1; and if the vehicle speed is between 5 and 12, $\boldsymbol{k_v}$ increases linearly from 0 to 1.

(3) If the braking intensity z is too high, to ensure the safety of braking, regenerative braking should be suitably reduced or even withdrawn. Based on this, a correction coefficient $\boldsymbol{k_z}$ is introduced.

In summary, the regenerative braking force can be expressed as follows:

$$F_m=\begin{cases}\min\{F_f,F_{avaliable},\dfrac{T_{reg}}{r}\}\cdot k_{SOC}\cdot k_v\cdot k_z & \mathrm{z}<\mathrm{z}_A\\ \min\{k_{reg}\cdot F_f,F_{avaliable},\dfrac{T_{reg}}{r}\}\cdot k_{SOC}\cdot k_v\cdot k_z & \mathrm{z}\ge\mathrm{z}_A\end{cases}. \tag{17}$$

5. Co-simulation Based on AVL CRUISE and MATLAB/Simulink

5.1 Relationship between the Required Blocking Current and the Brake Pedal Opening

The brake model built using AVL CRUISE software is a disc brake based on the hydraulic principle: the brake pressure is selected based on the opening degree of the brake pedal, to obtain the required brake torque. The relationship between the brake oil pressure and the brake pedal opening is represented in Fig. 10. The relationship between the required braking torque and the oil pressure is expressed as follows:

$$T_b = 2p_b \cdot A_b \cdot \eta_b \cdot \mu_b \cdot r_b \cdot c_b, \tag{18}$$

where T_b is the required braking torque, expressed in N·m; A_b is the area of the brake piston, in m^2; P_b is the braking pressure that is required by the current brake, in pa; η_b is the braking efficiency of the brake; μ_b is the frictional coefficient of the brake; r_b is the effective friction radius of the brake, in m; and c_b is a specific braking factor.

By comparing the built EMB actuator model with the hydraulic disc brake model built using AVL CRUISE software, a one-to-one correspondence between the required locked-rotor current of the EMB actuator and the brake pedal opening in the braking process is identified, as illustrated in Fig. 11. Then, the EMB modelling using AVL CRUISE software can be completed on the basis of the mechanical hydraulic brake model.

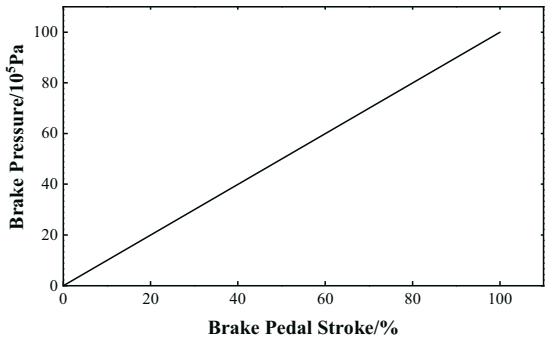

Fig. 10 Brake pedal stoke vs. brake pressure

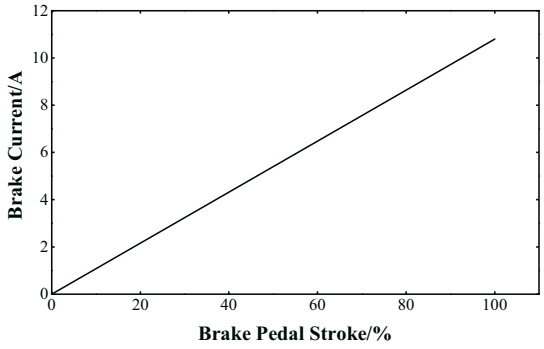

Fig. 11 Brake pedal stoke vs. brake current

5.2 Determination of the Model of Braking Strength

The braking strength characterizes the braking deceleration of an electric vehicle during braking. The braking strength can be expressed as follows:

$$z = \frac{T_b}{mgr}. \tag{19}$$

According to the relationship between the brake pedal opening and the required locked-rotor current, the required locked-rotor currents that correspond to various brake pedal openings in real time can be determined so that the required braking torque can be obtained and the braking strength z under the current braking road condition can be calculated as follows:

$$z = \frac{19.56\pi\eta_s\eta_b\eta_g R_b\mu_b c_b i_g k_e I_a}{P_h mgr}. \tag{20}$$

For the following simulation calculation, a SIMULINK model, as illustrated in Fig. 12, is obtained on the basis of the proposed control strategy and the identification model of the brake strength z. In addition, the vehicle model built using AVL CRUISE is illustrated in Fig. 13.

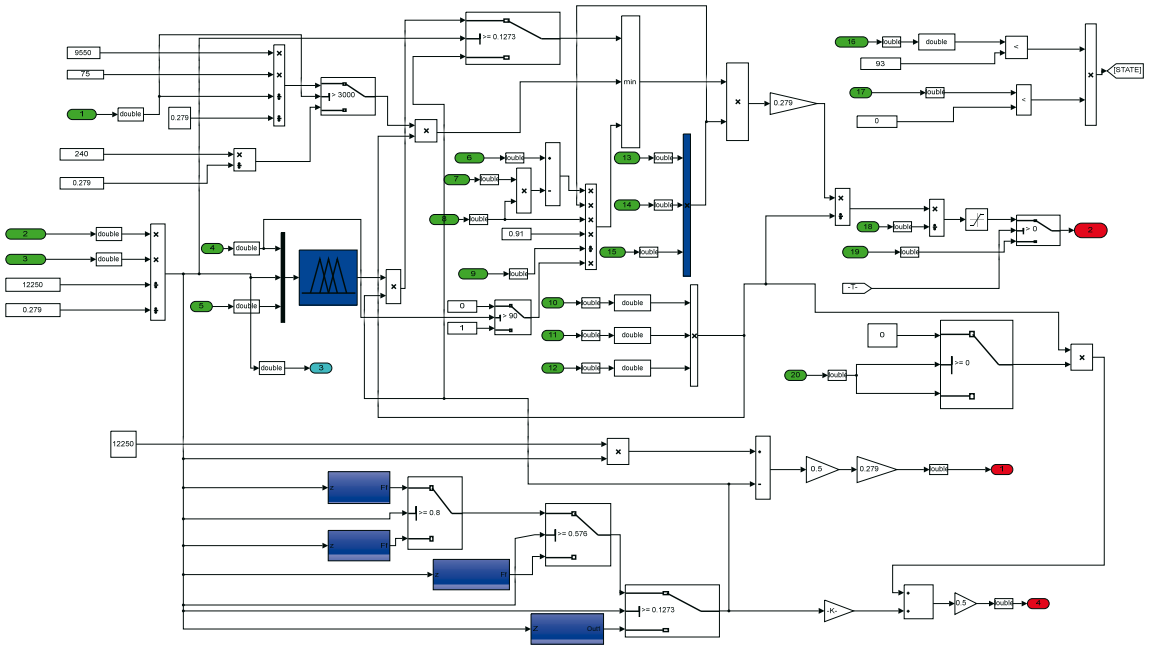

Fig. 12 Simulink Model of the Control Strategy

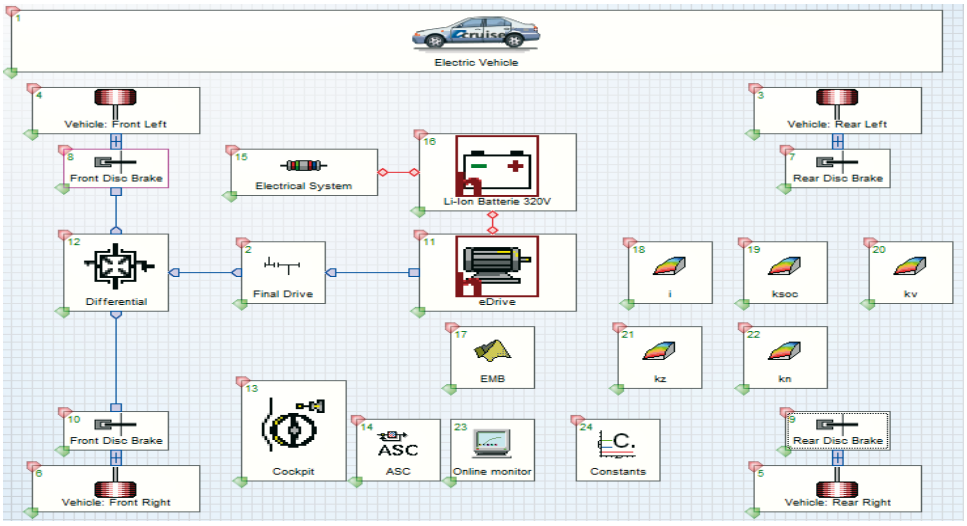

Fig. 13 Vehicle Model

5.3 Simulation Results

To evaluate the fuzzy control strategy based on the EMB proposed above, the *MATLAB_DLL method* is used for integrated simulation analysis. Through the built-in compiler of Simulink, the control strategy can be converted into the offline dynamic link library file (dll file) for subsequent joint simulation. In the AVL CRUISE, the dll file of the control strategy mentioned above is added into the dll module of the built pure electric model. Finally, the whole vehicle data bus is connected and the working conditions are set to carry out joint simulation. The basic parameters of the whole vehicle and the simulation data needed by some modules are specified in Table 1.

To accurately simulate the braking process of a pure electric vehicle, light braking and moderate braking conditions are defined. Relevant indicators of braking conditions are listed in Table 2.

The energy recovered in the braking process can be calculated via the following equation from the increment of the battery SOC:

$$E_{reg} = \Delta SOC \cdot U_N \cdot Q_N \cdot 3600, \tag{21}$$

where ΔSOC is the increment of SOC during braking, in %; U_N is the voltage of the battery, in V; and Q_N is the capacity of a battery, in A·h.

Table 1 Simulation data

Parameter	Unit	Value
Vehicle weight m	kg	1250
Gravitational acceleration g	m/s^2	9.8
Centroid height h_g	M	0.52
Wheelbase L	m	2.4
Distance from the centroid to the rear axle L_b	m	1.25
Distance from the centroid to the front axle L_a	m	1.15
Wheel radius r	m	0.279
Maximum torque of the motor N_{max}	(N·m)	240
Maximum motor power P_{max}	kW	75
Battery nominal voltage U_N	V	320
Battery capacity Q_N	(A·h)	120

Table 2 Braking conditions

Braking condition	Initial vehicle speed /(km/h）	Coefficient of adhesion	Initial SOC/%
Mild braking condition	30	0.8	50
Moderate braking condition	80	0.8	50

The energy that can be recovered during braking can be calculated using the kinetic energy theorem as expressed in equation (22), and the energy recovery and utilization rate can be calculated via equation (23) [29]:

$$E = \frac{1}{2} m \Delta v^2 \tag{22}$$

$$\eta_{reg} = \frac{E_{reg}}{E}. \tag{23}$$

The distributions of the braking force during mild braking and moderate braking are respectively represented in Fig. 14 and Fig. 15. According to Fig. 14 and Fig. 15, the trend of mechanical braking force and electric braking force changing with time is obviously different under different braking conditions.

Under light braking conditions, to more accurately simulate the braking process, the car is set to start braking at an initial speed of 30 km/h with variable braking strength. According to Fig. 16, the electric vehicle begins to decelerate and brake at an initial speed of 30 km/h and, finally, after 6 s, the speed of the electric vehicle becomes 0, during which the energy that the vehicle can recover is 43056.25 J according to the kinetic energy theorem. The initial SOC value of the car was set at 50% and after 6 seconds of braking it increased to 50.009%. According to equation (20), the recovered energy was 12,441.6 J and the energy recovery rate was the ratio of the above two quantities, namely 28.9%.

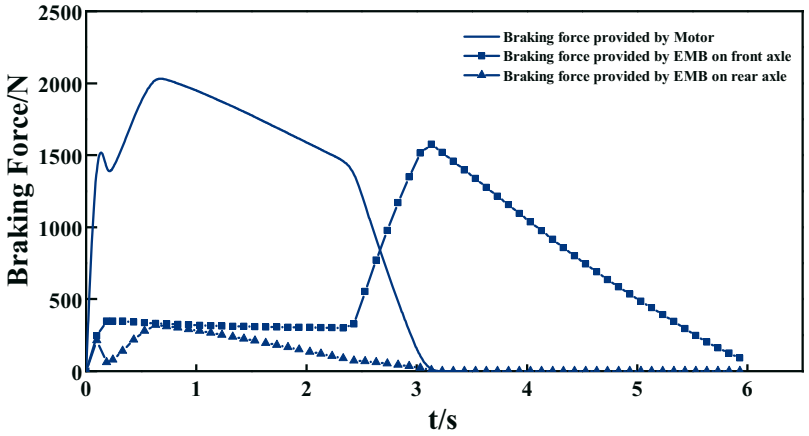

Fig. 14 Braking Force Distributions under Light Braking Conditions

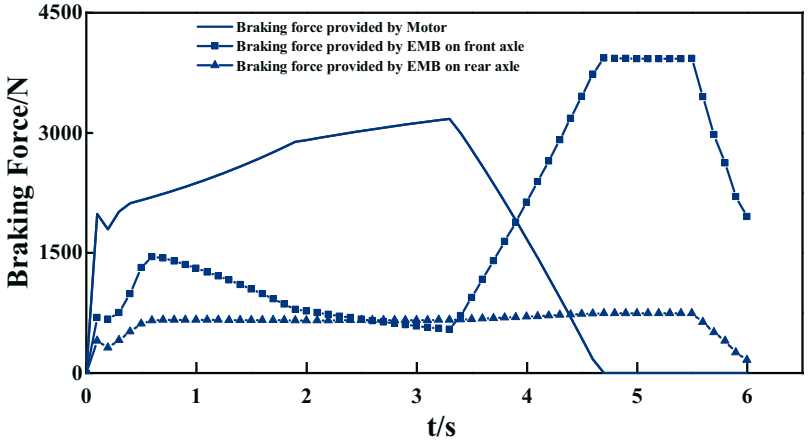

Fig. 15 Braking Force Distributions under Moderate Braking Conditions

Similarly, to more accurately simulate the scenario of moderate braking, the initial braking strength is set to 0.6. As can be seen from **Fig. 17**, under moderate braking, from the initiation of braking at the initial speed of 80 km/h to stopping, the recoverable energy is 308,025 J, the recovered energy is 105,062.4 J, and the recovery efficiency is 34.11%.

To further evaluate the economic performance of the vehicle under this control strategy, the constructed vehicle model will be simulated and analysed under New European Driving Cycle (NEDC) conditions. In addition, it is compared with a series control strategy on the basis of the ideal curve of the front and rear axle braking force distribution. The simulation results are represented in Fig. 18. Through comparison, it is found that the decrease of SOC of the fuzzy control strategy proposed in this paper is substantially delayed. Under the condition that the pure electric vehicle used for the simulation employs the same mechanism parameters and under the NEDC, the fuzzy control strategy put forward above reduces the power consumption over 100 kilometres by 4.9% compared with the series control strategy on the basis of the ideal curve.

In order to further evaluate the pros and cons of the control strategy proposed here, the vehicle model is simulated and the two control strategies are analysed under the US06 driving cycle - Supplemental Federal Transportation Procedure (FTP) Driving Schedule. First of all, it is necessary to import this new driving condition in CRUISE according to its driving schedule. The simulation result is shown in Figure 19. Through comparison, it is clear that under such high-speed and high-acceleration driving conditions, the fuzzy control strategy put forward in this paper can make the vehicle recover more braking energy. When the parameters are the same, the SOC reduction of the fuzzy control strategy suggested above is greatly delayed. After the US06 cycle, the SOC value of the vehicle based on the fuzzy control strategy is reduced by

8.44%, while the SOC value of the vehicle based on the I curve is reduced by 9.28%. The results make it clear that the fuzzy control strategy designed above has more advantages in terms of vehicle braking energy recovery under such more intense cycle conditions.

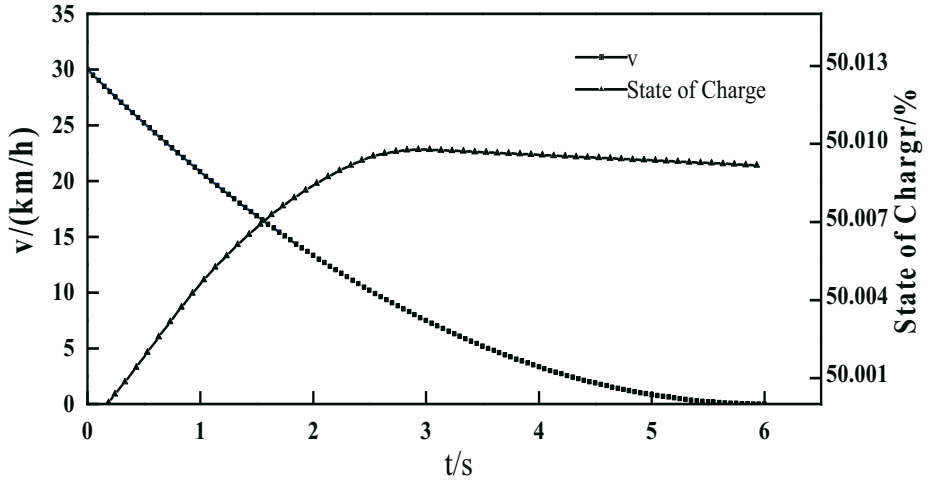

Fig. 16 Simulation Results under Light Braking Conditions

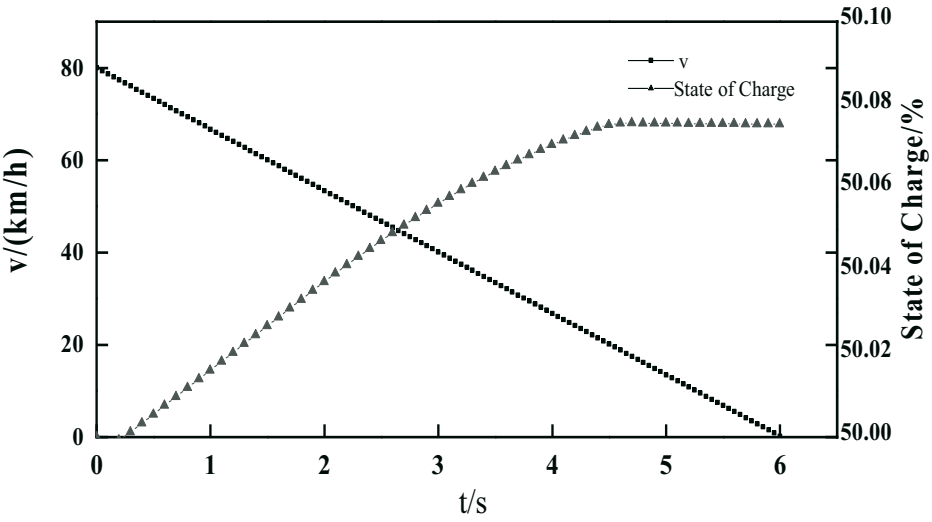

Fig. 17 Simulation Results under Moderate Braking Conditions

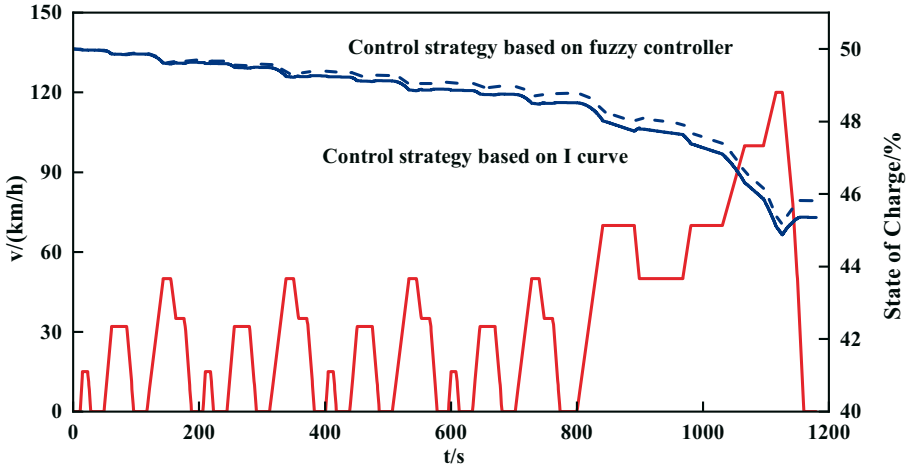

Fig. 18 Simulation Results under the NEDC

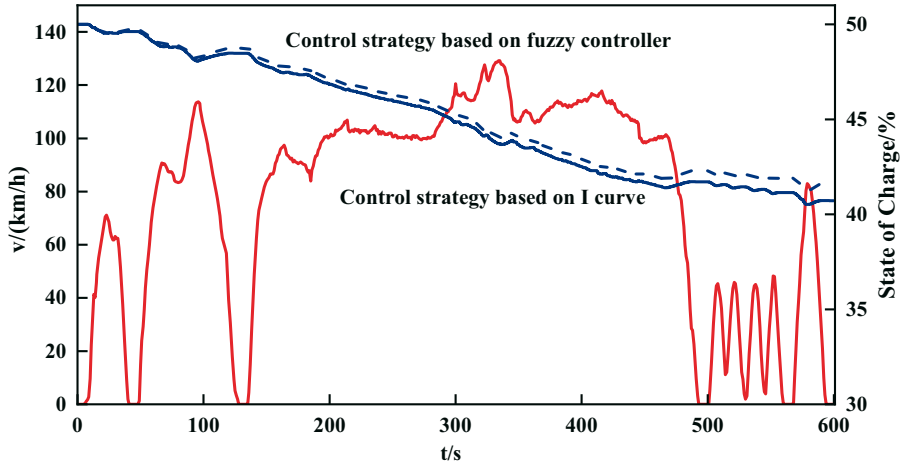

Fig. 19 Simulation Results under the US06

6. Conclusions

(1) According to the selected vehicle type, the operating characteristics of EMB, and the braking requirements of the whole vehicle, the regenerative braking system model of a pure electric vehicle equipped with EMB was designed. In addition, the structure of a kind of improved electromechanical brake was put forward, its working principle and performance advantages were introduced, and its mathematical model was established.

(2) Based on the braking safety area formed by the I curve, the ECE regulation line, the f curve and x-axis, a piecewise control strategy was proposed, which is used to specifically allocate the braking force between the axles. A fuzzy controller was used to obtain a proportion of regenerative braking. In consideration of the performance characteristics of the battery and motor, the obtained regenerative braking force was further modified combined with the three limiting factors v, SOC, and z. The one-to-one correspondence between the locked-rotor current required by the actuator of the EMB and the brake pedal opening was determined. Combined with the parameters of the selected vehicle, the dll files of the simulation models of EMB and the braking force distribution strategy were added to the specified module of the pure electric vehicle model established in CRUISE, and the co-simulation was performed.

(3) The simulation results showed that the braking energy recovery rate was 28.9% under light braking conditions, and 34.11% under moderate braking conditions. In contrast with the series control strategy on the basis of the ideal curve, the fuzzy control strategy presented in this paper can reduce the power consumption over 100 kilometres by 4.9% under NEDC conditions. The results show that the control strategy proposed here can further improve the energy utilization rate and extend the driving range of vehicles.

Acknowledgements

This work is partially supported by the National Natural Science Foundation of China (Grant No. 51205051).

REFERENCES

[1] Reif, K. Fundamentals of automotive and engine technology, *Springer* 2014, Wiesbaden. https://doi.org/10.1007/978-3-658-03972-1

[2] Day, A.J. Braking of road vehicles, *Butterworth-Heinemann* 2014, Oxford.

[3] Liu, W. Introduction to hybrid vehicle system modeling and control, *John Wiley & Sons* 2013, Hoboken.

[4] Ferreira, A.A.; Pomilio, J.A.; Spiazzi, G.S. Energy management fuzzy logic supervisory for electric vehicle power supplies system, *IEEE Transactions on Power Electronics* 2008, 23(1), 107-115. https://doi.org/10.1109/TPEL.2007.911799

[5] Bai, Z.F.; Li, S.X.; Cao, B.G. H∞ Control applied electric torque control for regenerative braking of an electric vehicle, *Journal of Applied Sciences* 2005, 5(6), 1103-1107. https://doi.org/10.3923/jas.2005.1103.1107

[6] Fazeli, A.; Zeinali, M.; Khajepour, A. Application of adaptive sliding mode control for regenerative braking torque control, *IEEE/ASME Transactions On Mechatronics* 2011, 17(4), 745-755. https://doi.org/10.1109/TMECH.2011.2129525

[7] Saeks, R.; Cox, C.J.; Neidhoefer, J. Adaptive control of a hybrid electric vehicle, *IEEE Transactions on Intelligent Transportation Systems* 2002, 3(4), 213-234. https://doi.org/10.1109/TITS.2002.804750

[8] Sciarretta, A.; Back, M.; Guzzella, L. Optimal control of parallel hybrid electric vehicles, *IEEE Transactions on control systems technology* 2015, 12(3), 352-363. https://doi.org/10.1109/TCST.2004.824312

[9] Laldin, O.; Moshirvaziri, M.; Trescases, O. Predictive algorithm for optimizing power flow in hybrid ultracapacitor/battery storage systems for light electric vehicles, *IEEE Transactions on Power Electronics* 2013, 28(8): 3882-3895. https://doi.org/10.1109/TPEL.2012.2226474

[10] Khastgir, S. The simulation of a novel regenerative braking strategy on front axle for an unaltered mechanical braking system of a conventional vehicle converted into a hybrid vehicle, *2013 Eighth International Conference and Exhibition on Ecological Vehicles and Renewable Energies (EVER)* 2013, 1-6. https://doi.org/10.1109/EVER.2013.6521600

[11] Tian, S.P.; Lv, C.Y. Research on regenerative braking strategy of pure electric vehicles based on fuzzy control, *Techniques and Methods* 2018, 37(8), 92-97.

[12] Shi, Q.S.; Zhang, C.H.;C, N.X. A new type of electric vehicle regenerative braking force distribution strategy, *Electrical Technology Journal* 2007, 22(2), 291-295.

[13] Liu, Z.Q.; Guo, X.X. Electro-hydraulic composite regenerative braking control of pure EV, *Journal of Central South University*: *Science and Technology* 2011, 42(9), 2687-2691.

[14] Hwang, S.H.; Kim, H.S.; Jin, H.B. Analysis of a regenerative braking system for hybrid electric vehicles using an electro-mechanical brake, *International Journal of Automotive Technology* 2009, 10(2), 229-234. https://doi.org/10.5772/10183

[15] Zhou, Z.G.; Mi, C.; Zhang, G.X. Integrated control of electromechanical braking and regenerative braking in plug-in hybrid electric vehicles*, International Journal of Vehicle Design* 2012, 58(2), 223-239. https://doi.org/10.1504/IJVD.2012.047381

[16] Wang, G.Y.; Zhang, J.L.; Xiao, H. Energy regenerative braking feedback lockup electromechanical integrated brake system for vehicles, *Applied Mechanics and Materials* 2012, 1503(264), 332-338. https://doi.org/10.4028/www.scientific.net/AMM.130-134.332

[17] Kim, J.; Jo, C.; Kwon, Y. Electro-mechanical brake for front wheel with back-up braking, *SAE International Journal of Passenger Cars - Mechanical Systems* 2014, 7(4), 1369-1373. https://doi.org/10.4271/2014-01-2538

[18] Chen, Y.; Bei, S.Y.; Wang, W. Research on the braking energy recovery system of electric vehicle based on EMB and EBD, *Modern Manufacturing Engineering* 2016, 12(12), 62-66.

[19] Shen, C.; Wang, J.; Li, Y. Study on brake actuator of electro-mechanical braking system, *Transactions of the Chinese Society for Agricultural Machinery* 2007, 38(8), 30-33.

[20] Sun, Y.T.; Wang, Y.L.; Zhu, R.F. Study on the control strategy of regenerative braking for the hybrid electric vehicle under typical braking condition, *IOP Conference Series: Materials Science and Engineering*, 2018, 452(3), 032092. https://doi.org/10.1088/1757-899X/452/3/032092

[21] Nelson, R. From line-voltage simulation to regenerative braking test, *EE: Evaluation Engineering: The Magazine of Electronic Evaluation* 2018, 57(9), 6-11.

[22] Ye, M.; Guo, J.G. Electric vehicle regenerative braking and its control technology, *China Communications Press* 2013, Beijing.

[23] Yu, Z.S. Automobile theory, *Mechanical Industry Press* 2009, Beijing.

[24] Liu, L.J.; Ji, F. J.S.; Yang, C. Control strategy for electro-mechanical braking based on curves of ECE regulations and ideal braking force, *Journal of Beijing University of Aeronautics and Astronautics* 2013, 39(1), 138-142.

[25] Li, S.Q.; Yu, B.; Feng, X.Y. Research on braking energy recovery strategy of electric vehicle based on ECE regulation and I curve, *Science Progress* 2020, 103(1), 1-17. https://doi.org/10.1177/0036850419877762

[26] Fazeli, A. Application of adaptive sliding mode control for regenerative braking torque control, *IEEE/ASME Transactions on Mechatronics* 2012, 17(4), 745-755. https://doi.org/10.1109/TMECH.2011.2129525

[27] Zhou, S.W.; Wang, Q.Y. Simulation research on regenerative braking control strategy of electric vehicle, *IOP Conference Series: Materials Science and Engineering* 2019, 657(2019). https://doi.org/10.1088/1757-899X/657/1/011001

[28] Wang, M.Z.; Sun, C.; Zhuo, G.R. Braking energy recovery system for electric vehicle, *Transactions of the Chinese Society for Agricultural Machinery* 2012, 43(2), 6-10.

[29] Yang, H.S.; Ji, F.Z.; Yang, S.C. Research of braking energy recovery system based on Simulink-Cruise combined simulation, *Control Engineering of China* 2018, 25(6), 1086-1090.

Submitted: 06.6.2020

Accepted: 11.02.2022

Shuwen Zhou
Qingyun Wang*
Jinshuang Liu
College of Mechanical Engineering and Automation, Northeastern University, Shenyang Liaoning 110819, China
*Corresponding author:
qingyunwang@tom.com